

CONTROL STRATEGY OF SWITCHING REGULATORS FOR PHOTO VOLTAIC POWER APPLICATIONS

P.KALPANA¹, DR.S.SIVA PRASAD²

¹PG Scholar, Vidya Jyoti Institute of Technology, Hyderabad, TS, India.

²Professor & HOD of EEE Dept., Vidya Jyoti Institute of Technology, Hyderabad, TS, India.

ABSTRACT-Usually accepted that the input voltage source of a switch-mode power supply is constant or shows insignificant small variations. In any case, the last assumption is not any more valid when an PV is utilized as input source. A PV is described by low and unregulated DC output voltage, moreover, this voltage diminishes in a non-linear form when the demanded current increments; from now on, an appropriate controller is required to adapt the previously mentioned issues. In this investigation, a normal current-mode controller is planned utilizing a joined model for an energy unit PV and a boost converter; besides, a determination method for the controller picks up guaranteeing system stability and output voltage regulation is produced. The proposed energy system utilizes an energy component power module and a boost converter conveying a power of 900 W. Simulation results affirm the proposed controller execution for output voltage regulation by means of closed loop gain estimations and step load changes. What's more, a correlation amongst open-and closed-loop estimations is made, where the controller robustness is tried for vast load varieties and PV stack output voltage changes also.

1 INTRODUCTION

Photovoltaics offer consumers the ability to generate electricity in a clean, quiet and reliable way. Photovoltaic systems are comprised of photovoltaic cells, devices that convert light energy directly into electricity. Because the source of light is usually the sun, they are often called solar cells. The word photovoltaic comes from "photo," meaning light, and "voltaic," which refers to producing electricity. Therefore, the photovoltaic process is "producing electricity directly from sunlight." Photovoltaics are often referred to as PV.

PV cells convert sunlight directly into electricity without creating any air or water pollution. PV cells are made of at least two layers of semiconductor material. One layer has a positive charge, the other negative. When light enters the cell, some of the photons from the light are absorbed by the semiconductor atoms, freeing electrons from the cell's negative layer to flow through an external circuit and back into the positive layer. This flow of electrons produces electric current. To increase their utility, dozens of individual PV cells are

interconnected together in a sealed, weatherproof package called a module. When two modules are wired together in series, their voltage is doubled while the current stays constant. When two modules are wired in parallel, their current is doubled while the voltage stays constant. To achieve the desired voltage and current, modules are wired in series and parallel into what is called a PV array. The flexibility of the modular PV system allows designers to create solar power systems that can meet a wide variety of electrical needs, no matter how large or small.

A grid-connected PV system will require a utility interactive DC to AC inverter. This device will convert the direct current (DC) electricity produced by the PV array into alternating current (AC) electricity typically required for loads such as radios, televisions and refrigerators. For an off-grid PV system, consumers should consider whether they want to use the direct current (DC) from the PV's or convert the power into alternating current (AC). Appliances and lights for AC are much more common and are generally cheaper, but the conversion of DC power into AC can consume up to 20 percent of all the power produced by the PV system.

2 COMBINED PV STACK/BOOST CONVERTER MODEL

A PV is heat -based electrical energy source that generates low and unregulated DC voltage, where the output voltage decreases in a non-linear fashion when the demanded current increases. The stack output voltage terminals are connected to a DC/DC power converter to finally provide a voltage required to feed either a DC or a AC load. In the following, an overall mathematical description capturing precisely the coupling between the PV and a DC/DC boost converter is shown in detail.

2.1PV Static Properties

Several expressions have been proposed in the open literature to predict the heat and thermal dynamical behavior of PV. However, for the purpose of this work, a suitable and easy-to-handle PV expression including electric properties compatible with power conversion is used. For instance, a PV static expression for the output voltage which

depends on the output current and physical parameters is given in where V_{PV} is the PV output voltage, I_{PV} is the PV current and E_o is the open-circuit voltage.

$$v_f(i_f) = \frac{E_o}{1+(i_f/I_h)^\delta} \quad (1)$$

The parameters δ and I_h depend on the environment humidity conditions and stack temperature. These parameters together with E_o are required to be computed for a given PV. A N_{exa} module is used and characterised in this work.

Remark 1: The expression that represents the static properties of the PV (1) was taken from; however, a methodology is required to obtain (from available measured data) the parameters δ and I_h . In the following, an explanation about the computation of the parameters E_o , δ and I_h is given. A set of N discrete experimental samples ($i_{f \text{ exp}(k)}$, $v_{f \text{ exp}(k)}$) with $k = 1, 2, 3, \dots, N$, corresponding to the stack output current and voltage are required. In this case, the samples are depicted in circles in Fig. 1a.

$$\left(\frac{i_f}{I_h}\right)^\delta = \frac{E_o}{v_f} - 1 \quad (2)$$

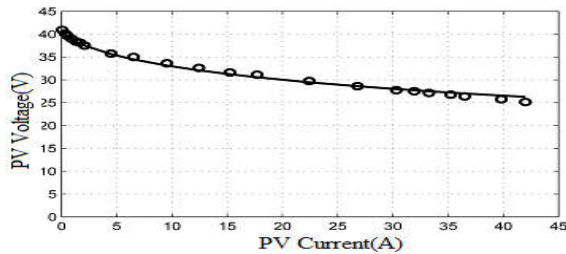


Fig. 1 PV/boost converter system (a) Nexa power module static output characteristics, data (circles), model (solid line),

and recalling some basic logarithm properties, (2) can be expressed as

$$\delta \log i_f - \delta \log I_h = \log \left(\frac{E_o}{v_f} - 1\right) \quad (3)$$

Assuming that (3) holds for all recorded samples ($i_{f \text{ exp}(k)}$, $v_{f \text{ exp}(k)}$) with E known, then (3) has the form

$$a_1 x + a_0 = y \quad (4)$$

Where

$$a_1 = \delta; x = \log i_f; a_0 = -\delta \log I_h; y = \log \left(\frac{E_o}{v_f} - 1\right) \quad (5)$$

Finally, using the well-known linear least square data fitting, the parameters δ and I_h can be obtained from the following computations (all sums are of the form $\sum_{k=1}^N$):

$$x_k = \log(i_{f \text{ exp}(k)});$$

$$y_k = \log\left(\frac{E_o}{v_{f \text{ exp}(k)}} - 1\right);$$

$$a_0 = \frac{\sum x_k^2 \sum y_k - \sum x_k y_k \sum x_k}{N \sum x_k^2 - (\sum x_k)^2} \quad (6)$$

Which yield to

$$\delta = \frac{N \sum x_k y_k - \sum x_k \sum y_k}{N \sum x_k^2 - (\sum x_k)^2} = 0.64,$$

$$I_h = \log^{-1}\left(-\frac{a_0}{\delta}\right) = 82.86 \quad (7)$$

for $N = 22$ samples and $E_o = 41.7$ V. A comparison between experimental data and the expression in (1) is given in Fig. 1a, which confirms the accuracy of the described method. In addition, this static model (1) is continuous for a large range of currents, including no current and maximum current.

2.2 Overall mathematical representation

The proposed physical implementation of the PV/boost converter system is shown in Fig. 1b, where Q is the active switch [metal-oxide-semiconductor field-effect transistor (MOSFET)], u the duty cycle, D the diode, L the filter inductor, C the filter capacitor and R the load resistance. Subsequently, i_f , i_{Cf} , i_L , i_c and i_o are the average PV, coupling capacitor, inductor, capacitor and output currents, respectively.

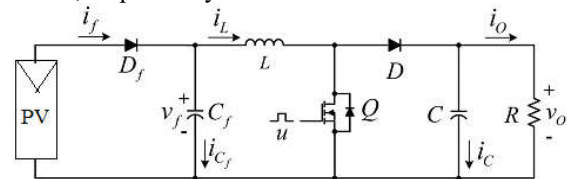


Fig. 1 PV/boost converter system (b) PV/boost converter system

The dynamic behaviour of many classes of power circuits are analyzed using the notion of average models, which can be manipulated using standard circuit techniques. Average models can be derived for high-frequency switching converters, where linearization can be easily carried out. In this sense, using Kirchhoff laws when Q is ON/OFF and the current i from (2), the average (ripple-free) continuous non-linear model is obtained as

$$\dot{v}_f = \frac{1}{C_f} \left(I_h \left(\frac{E_o}{v_f} - 1\right)^\delta - i_L \right),$$

$$i_L = \frac{1}{L} (v_f - (1-u)v_o),$$

$$\dot{v}_o = \frac{1}{C} \left((1-u)i_L - \frac{v_o}{R} \right) \quad (8)$$

Where the state vector is $[v_f, i_L, v_o]^T \in \mathbb{R}^+ + 3$ and the input $u \in (0, 1)$. The non-linear differential equations in (8) are said to be bilinear, since the input signal u is multiplying the state variables v_o and i_L directly.

Remark 2:

A link capacitor is connected in between the PV and the boost converter, meanwhile [27] uses a series inductor for the same task. In steady state, the

average output voltage V_O is greater than the input V_{PV} , also the inductor current I_L equals to the PV current I_{PV} ; therefore, the nominal operating conditions of (8) are found to be

$$V_O = \frac{V_f}{1-U}, I_L = \frac{V_O}{R(1-U)} = I_h \left(\frac{E_o}{v_f} - 1 \right)^{1/\delta} \quad (9)$$

Once the nominal output voltage V_O is defined, the resulting PV voltage V_{PV} can be computed from the numerical solution of

$$V_f + \frac{V_O^{\delta}}{(RI_h)^{\delta}} V_f^{1-\delta} - E_o = 0 \quad (10)$$

Note that ideal components and zero voltage losses are assumed in (8)–(10); therefore, the numerical results may differ from those in practice. Furthermore, in steady-state CCM operation, the voltage and current ripples for the boost converter due to the switching action can be computed by

$$\Delta V_O = \frac{I_o U}{C f_s}, \Delta I_o = \frac{V_f U}{L f_s} \quad (11)$$

additionally, to ensure CCM, the inductor value must be selected as

$$L > \frac{U(1-U)^2 R}{2 f_s} \quad (12)$$

yields to the linear average small-signal model for the overall system as

$$\begin{bmatrix} \dot{\tilde{v}}_f \\ \dot{\tilde{i}}_L \\ \dot{\tilde{v}}_0 \end{bmatrix} = \begin{bmatrix} -\frac{1}{C_f k} & -\frac{1}{C_f} & 0 \\ \frac{1}{L} & 0 & -\frac{1-U}{L} \\ 0 & \frac{1-U}{C} & -\frac{1}{RC} \end{bmatrix} \begin{bmatrix} \tilde{v}_f \\ \tilde{i}_L \\ \tilde{v}_0 \end{bmatrix} + \begin{bmatrix} 0 \\ \frac{V_o}{L} \\ -\frac{I_L}{C} \end{bmatrix} \tilde{u} \quad (13)$$

where the new state vector is $[\tilde{v}_f, \tilde{i}_L, \tilde{v}_0]^T \in \mathbb{R}^3$ and

$$k = \frac{E_o \delta I_h^{\delta} I_f^{\delta-1}}{(I_h^{\delta} + I_f^{\delta})^2} \quad (14)$$

The resulting model (14) combines two subsystems dynamics and has only one input $u \sim \in \mathbb{R}$. This linear time-invariant model describes approximately the behaviour of the PV/boost converter system for frequencies up to half of the switching frequency f_s . Furthermore, it can be used for analysis and controller design of switching regulators.

3. AVERAGE CURRENT-MODE CONTROLLER

Average CMC is a useful technique for easing the design and improving the dynamic performance of switch-mode converters. Here, a methodology to properly select the controller gains for stability and performance purposes is provided. Additionally, sensing the inductor current can also be used for preventing overload current through the converter. This control technique uses a high-gain

compensator, a low-pass filter and a PI controller to warrant: (i) that the average inductor current follows the current reference, and (ii) output voltage regulation.

The advantage of this approach is that any change in the input voltage source has an immediate effect in the controller (fast propagation property). The overall controller design procedure is a twofold problem: (i) gain selection for the current loop, and (ii) gain selection for the voltage loop. In order to derive the controller expressions, a configuration for this technique is proposed in Fig. 2.

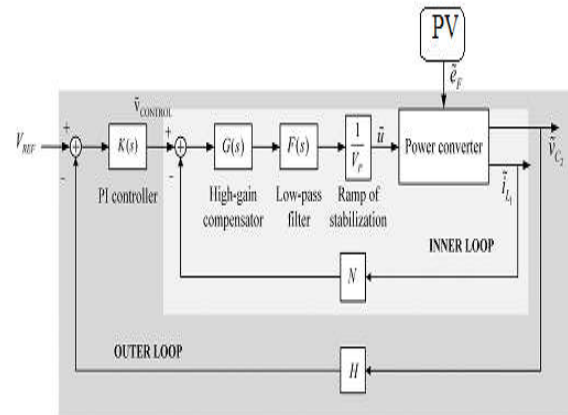


Fig. 2 Average CMC scheme for a switching regulator

Remark 3:

The control scheme proposed in has two control loops for output voltage regulation as well, but the high-gain compensator and the low-pass filter are integrated to the voltage loop, meanwhile the current loop is implemented by a hysteresis controller. For robust stability of each loop, the following requirements have to be satisfied:

- for relative stability, the slope at or near cross-over frequency must be not more than -20 dB/dec;
- To improve steady-state accuracy, the gain at low frequencies should be high;

3.1 Current Loop

The control law $u \sim$ is defined by

$$\tilde{u} = \frac{1}{V_P} \underbrace{\left(\frac{1}{1+(s/\omega_p)} \right)}_{F(s)} \underbrace{\left(G_P \frac{(s/\omega_z)+1}{s/\omega_z} \right)}_{G(s)} (I_{ref} - N i_L) \quad (15)$$

Where ω_p stands for the location of the filter pole, G_P is the compensator gain, ω_z is the location of the compensator zero and I_{ref} is the output of the voltage loop. Note that both transfer functions $F(s)$ and $G(s)$ can be implemented using a single operational amplifier as shown in Fig. 3.

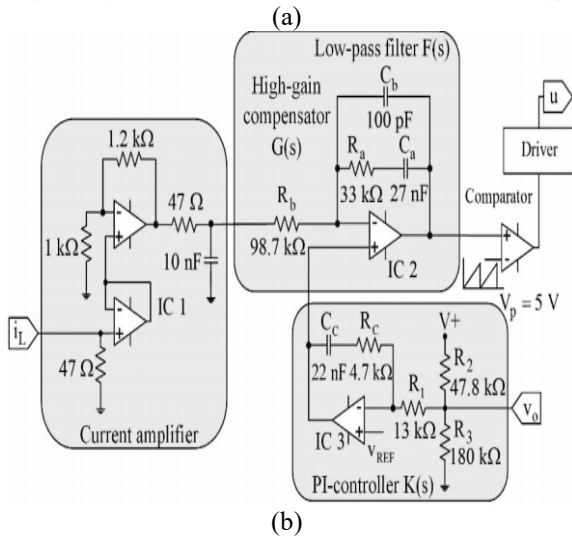
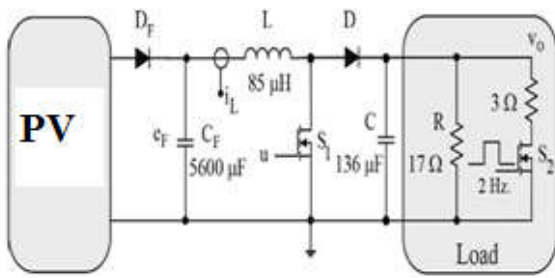


Fig. 3 Switching regulator (a) Combined PV /boost converter, (b) Average current-mode controller

The zero ω_Z of the high-gain compensator should be placed at least a decade below of half of the PWM switching frequency, $f_s/2$. Practically, the zero is determined by the relationship

$$\omega_Z = \frac{1}{R_a C_a} \quad (16)$$

Where R_a and C_a are the resistance and capacitance corresponding to the current loop control circuit.

The pole ω_P of the low-pass filter, on the other hand, should be placed either at $f_s/2$ or above. Using the circuitry in Fig. 4, the pole is determined by

$$\omega_P = \frac{C_a + C_b}{R_a C_a C_b} \quad (17)$$

where C_b is the capacitor associated to the current loop circuit as well.

The compensator gain is computed by

$$G_P = \frac{R_a}{R_b} \quad (18)$$

where the resistance values must be carefully selected such that

$$G_P < \frac{5(1-U)^2 R}{N V_0} \quad (19)$$

3.2 Voltage Loop

The outer loop should be designed to provide a suitable steady state correction of the

output voltage and can be implemented using a PI controller. The output of this loop is the current reference

$$I_{ref} = \frac{K_C (1 + (1/T_i s)) (V_{ref} - H v_o)}{K(s)} \quad (20)$$

Where K_C is the proportional gain, T_i is the integral time and V_{ref} is the reference output voltage. In this case, the selection criteria should follow:

The proportional gain $K_P = RC/R_1$ is selected such that

$$K_P < \frac{10(1-U)}{H V_0} \quad (21)$$

where the voltage divider is

$$H = \frac{R_1 R_3}{R_1 R_3 + R_2} \quad (22)$$

Finally, the integral time is computed from

$$T_i = R_C C_C \quad (23)$$

Where R_C and C_C are the resistance and capacitance values of the PI controller circuit, which must be selected such that $1/T_i$ is placed at least one decade below f_s .

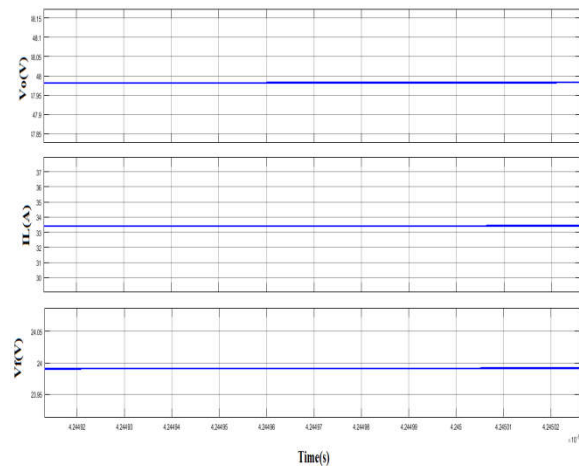
Remark 4:

In contrast to VMC, here an inner loop is added. This improves significantly the transient performance of the controller, since the transfer function $v \sim O/u \sim$ of a boost converter has a right half-plane zero, and a single voltage loop may not deal properly with this issue.

4. SIMULATION RESULTS

4.1 Open-Loop Test

The simulation open-loop time response of the system is shown in Fig. 4a. It is noticeable that the simulation results are close enough to the theoretical relation given in (9). Using the MOSFET S 2 (trigger voltage V_g), step changes of 2 Hz are applied to the output load which ranges from 2.56 to 17 Ω . The resulting output voltage V_O is shown in Fig. 4b, which changes for about 33 V. On the other hand, Fig. 4c shows the step changes on the PV side.



(a)

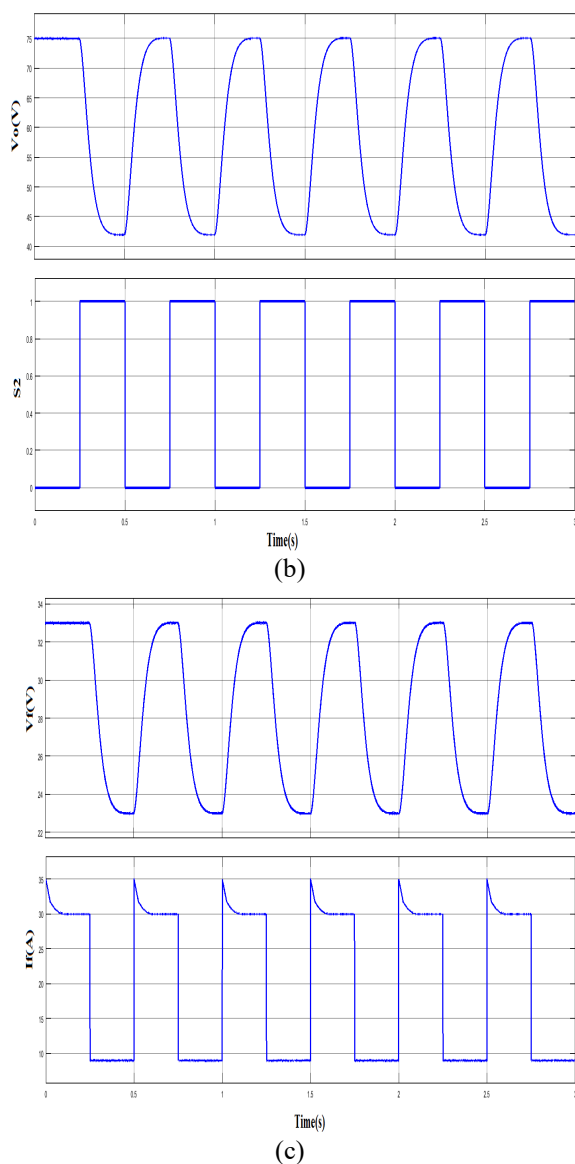
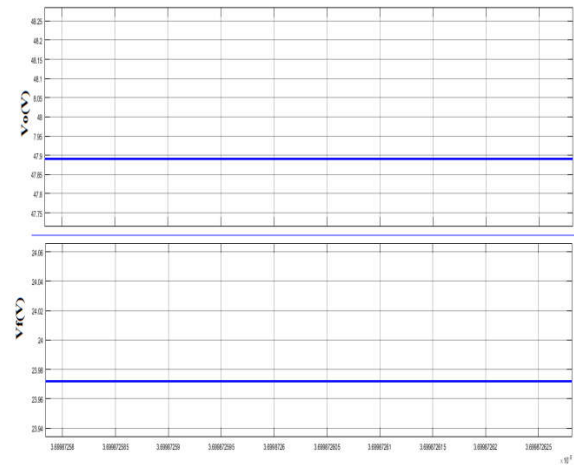


Fig. 4 simulation results in open-loop response for step changes in the load between 2.56 and 17 Ω (a) (From top to bottom) output voltage v_O (20 V/div), inductor current i_L (25 A/div) and PV voltage V_{PV} (20 V/div) (time: 10 μ s/div), (b) (From top to bottom) output voltage v_O (20 V/div) and gate voltage V_g of MOSFET S2 (20 V/div) (time: 200 ms/div), (c) (From top to bottom) output voltage of the PV V_{PV} (20 V/div) and output current of the PV I_{PV} (10 A/div) (time: 200 ms/div)

4.2 Closed-Loop Test

The switching regulator operating condition corresponding to 48 V output voltage at nominal load (no load changes) is shown in Fig. 5a. At this operating condition, the PV is delivering a voltage of 24 V. When output load changes are introduced, the resulting load voltage remains at 48 V

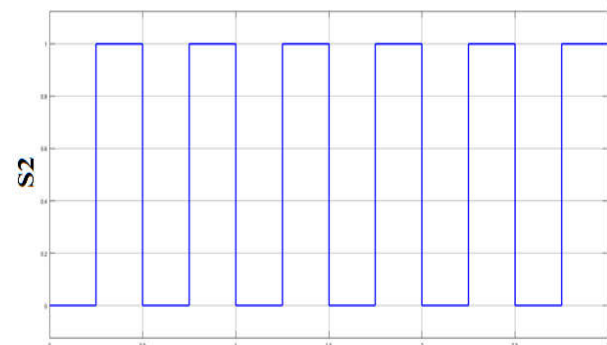
as shown in Fig. 5b, where it is clear the switching regulator is robust under large load variations. The demanded current ranges from 4 to 27 A, as is shown in Fig. 5c. This is due to the stored energy in the capacitor C_F that helps to compensate the changes in the demanded energy for closed-loop response. Note that the PV current in the open loop case (Fig. 4c) presents a 5A overshoot, meanwhile in the closed-loop case (Fig. 5c), the current does not present any overshoot; therefore, the life cycle of the PV is not overwhelmed. The current ripple is shown in Fig. 5d, which is small (1.2 A peak to peak) due to the capacitor C_F .



(a)



Time(s)



Time(s)
(b)

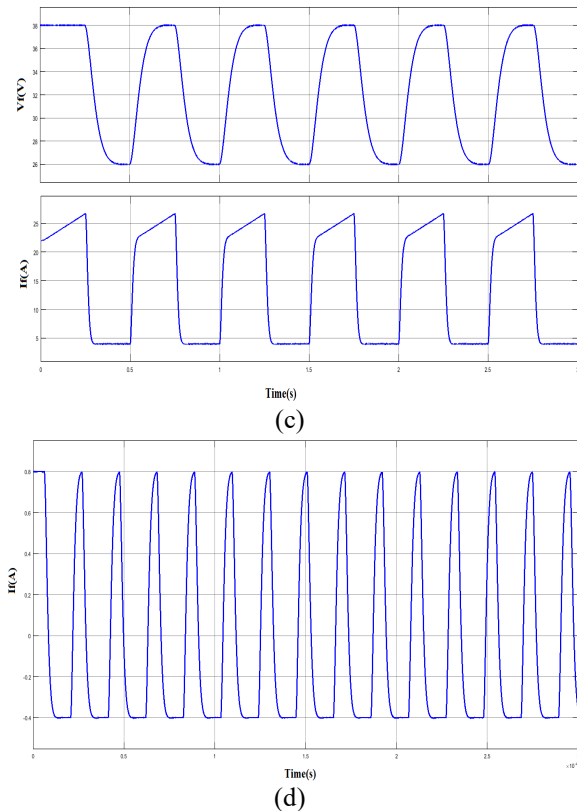


Fig. 5 Closed-loop response (a) Response at nominal load (2.56Ω). (From top to bottom) output voltage v_O (20 V/div) and PV voltage V_{PV} (20 V/div) (time: 200 ms/div), (b) Response to step changes in the load between 2.56 and 17Ω : (from top to bottom) output voltage v_O (20 V/div) and gate voltage V_g of MOSFET S2 (20 V/div) (time: 200 ms/div), (c) Response to step changes in the load between 2.56 and 17Ω : (from top to bottom) PV voltage V_{PV} (20 V/div), and output current of the PV I_{PV} (10 A/div) (time: 200 ms/div), (d) Output current ripple of the PV I_{PV} (1 A/div) (time: 10 μ s/div)

CONCLUSIONS

This paper manages the output voltage regulation of a power module stack/boost converter system. The proposed control methodology is based on all things considered CMC where two loops are executed, to be specific the internal loop where the inductor current is fed back utilizing a high gain compensator and a low-pass filter, and the external loop where the output voltage is fed back by means of a PI controller for steady-state error regulation. The determination technique for the controller parameters is unequivocally definite. The criteria given inside guarantee system stability and output voltage regulation. The poles and zeros for the controller are set mainly from the working switching frequency of the converter. Furthermore, because of the high-gain compensator of the inward loop, the

converter execution is less sensitive to parameter uncertainties and varieties of the PV voltage. This control technique was executed utilizing low cost operational amplifiers, reasonable for commercial applications. At long last, simulation results utilizing a boost converter model show great robustness to huge variations on the load.

REFERENCES

- [1] Carrasco, J.M., Garcia, L., Bialasiewicz, J.T., et al.: 'Power-electronic system for the grid integration of renewable energy sources', IEEE Trans. Ind. Electron., 2006, 53, (4), pp. 1002–1016
- [2] Benson, Ch.L., Magee, Ch.L.: 'On improvement rates for renewable energy technologies: solar PV, wind, capacitors, and batteries', J. Renew. Energy, 2014, 68, pp. 745–751
- [3] Shen, J.-M., Joul, H.-L., Wu, J.-C.: 'Transformerless three-port grid connected power converter for distribution power generation system with dual renewable energy sources', IET Power Electron., 2012, 5, (1), pp. 501–509
- [4] Jakhar, H., Soni, M.S., Gakkhar, N.: 'Historical and recent development of concentrating photovoltaic cooling technologies', Renew. Sustain. Energy Rev., 2016, 60, pp. 41–59
- [5] Bahceci, S., Fedakar, S., Yalcinoz, T.: 'Examination of the grid-connected polymer electrolyte membrane fuel cell's electrical behaviour and control', IET Renew. Power Gener., 2016, 10, (3), pp. 388–398
- [6] Rahmal, S.A., Varmal, R.K., Vanderheide, T.: 'Generalised model of a photovoltaic panel', IET Renew. Power Gener., 2014, 8, (3), pp. 217–229
- [7] Li, Q., Chen, W., Liu, Z., et al.: 'Active control strategy based on vector proportion integration controller for proton exchange membrane fuel cell grid-connected system', IET Renew. Power Gener., 2015, 9, (8), pp. 991–999
- [8] Thounthong, P., Davat, B., Rael, S., et al.: 'Fuel cell high-power applications', IEEE Ind. Electron. Mag., 2009, 3, pp. 32–46
- [9] Kabalo, M., Pairel, D., Blunier, B., et al.: 'Experimental evaluation of four phase floating interleaved boost converter design and control for fuel cell applications', IET Power Electron., 2013, 6, (2), pp. 215–226
- [10] Leel, J.-G., Choe, S.-Y., Ahn, J.-W., et al.: 'Modelling and simulation of a polymer electrolyte membrane fuel cell system with a PWM dc/dc converter for stationary applications', IET Power Electron., 2008, 1, (3), pp. 305–317.
- [11] Thounthong, P., Davat, B.: 'Study of a multi-phase interleaved step-up converter for fuel cell applications', Energy Convers. Manage., 2010, 51, pp. 826–832

[12] Naik, M.V., Samuel, P.: 'Analysis of ripple current, power losses and high efficiency of dc-dc converters for fuel cell power generating systems', Renew. Sustain. Energy Rev., 2016, 59, pp. 1080–1088



P.KALPANA Completed B.Tech in Electrical Engineering In 2014 From Jaya Prakash Narayan College of Engineering Dharmapur mahabubnagar Telangana, India And Pursuing M.Tech From Vidya Jyoti Institute Of Technology, Hyderabad. Affiliated To JNTUH, Hyderabad, Telangana, India. Area Of Interest Includes Power electronics.

E-Mail Id:punnakalpana@gmail.Com.



DR.S.SIVA PRASAD, Professor & HOD of EEE Dept. has awarded Ph.D. Electrical Engineering in 2012 (February) from J.N.T.UNIVERSITY HYDERABAD And had his M.Tech with specialization of Power Electronics in 2003.He has obtained his B.Tech Degree in Electrical and Electronics Engineering from S V University. He is having 19 years of Experience and currently working as Professor & HOD of EEE Dept. of Vidya Jyoti Institute of Technology, Aziz Nagar, Hyderabad, India. He received —Bharat Vibhushan Samman Puraskarl from —The Economic and Human Resource Development Associationl in 2013 and received Young Investigator Award in 2012. He has published about 60 technical papers in International and National Journals and Conferences and filed one patent. He is Life member of ISTE and member of IEEE. His Research areas include Power Electronics & Drives, PSD&FACTS Controllers.